International Journal of Pharmaceutics 409 (2011) 96–103

Contents lists available at ScienceDirect

International Journal of Pharmaceutics

journal homepage: www.elsevier.com/locate/ijpharm

Pharmaceutical micro-particles give amorphous sucrose higher physical stability

Joel Hellrup, Denny Mahlin*

Department of Pharmacy, Uppsala University, Uppsala, Sweden

ARTICLE INFO

Article history:
Received 16 September 2010
Received in revised form 28 January 2011
Accepted 21 February 2011
Available online 26 February 2011

Keywords:
Amorphous
Sucrose
Physical stability
Freeze-drying
Crystallization
Micro-particles

ABSTRACT

The aim of this study was to explore how pharmaceutical micro-sized filler particles affect the amorphous stability of sucrose in sucrose/filler particle composites produced by freeze-drying. Focus was put on the filler particles' properties crystallinity, hygroscopicity, hydrophobicity, and surface area, and their influence on physical stability of the amorphous phase. The micro-sized filler particles were examined with Blaine permeametry, gas adsorption, pycnometry, gravimetric vapour sorption, X-ray diffraction, and light microscopy before composites of sucrose and micro-sized filler particles were prepared by freeze-drying. The stability of the composites was examined with X-ray diffraction, differential scanning calorimetry (DSC), and microcalorimetry. All composites were amorphous and showed higher stability compared to pure amorphous sucrose, which was evident from a delay in heat and moisture-induced crystallization. However, calcium carbonate and oxazepam micro-sized filler particles lost their ability to stabilize the amorphous sucrose when exposed to humidity. The dry glass transition temperature (T_g) was higher for the composites, indicating the stabilization was mediated by a reduced molecular mobility of the amorphous phase.

1. Introduction

During recent years there has been an increasing interest in the properties of amorphous materials. The amorphous state plays a role in biotechnology, more specifically in the formulations of biologics, as amorphous sugars have proven to be useful as carriers in dry formulations of, for example, proteins (Roberts and Debenedetti, 2002) and microorganisms (Pehkonen et al., 2008). It has been shown that it is essential that the matrix becomes amorphous to preserve protein structure and function in the dry state (Izutsu and Kojima, 2002; Chatterjee et al., 2005). The potential to utilize the amorphous state for dissolution improvement has also been demonstrated (Hancock and Parks, 2000; Lindfors et al., 2006; Murdande et al., 2010), and is therefore attracting attention within formulation science since solubility is a substantial problem for many new candidate drugs. Amorphous domains in pharmaceutical formulations can also emerge due to amorphization of excipients and drugs when subjected to unit operations, such as milling (Willart and Descamps, 2008; Lin et al., 2009; Planinsek et al., 2010) and compaction (Okumura et al., 2006). This mechanical activation which leads to, at least partially, an amorphization may be the reason behind altered properties of processed material. The role of amorphous content in pharmaceutical powders for compactibility and powder flow properties has been reported (Vromans et al., 1987; Sebhatu and Alderborn, 1999; Ziffels and Steckel, 2010). Hence, there is an increasing awareness that a well-controlled formation of amorphous phases within pharmaceutical materials can be utilized to produce solid formulations with advantageous properties.

A major challenge when using amorphous materials is to overcome the physical instability with respect to crystallization (Hancock et al., 1995; Roberts and Debenedetti, 2002; Bhugra et al., 2008; Graeser et al., 2008). To implement amorphization as a tool in product development, the stability issues have to be addressed in order to attain products that are stable on storage. The general strategy to stabilize the amorphous state is to lower the molecular mobility of the amorphous phase by mixing with polymers to form solid dispersions (Shamblin et al., 1996; Berggren and Alderborn, 2003; Mahlin et al., 2006; Bhugra and Pikal, 2008; Rumondor et al., 2009; Schoug et al., 2009). It is becoming increasingly apparent that it is important to match the amorphous component with stabilizing polymer to obtain interactions, e.g., hydrogen bonding, between the components to achieve a better stabilizing effect (Konno and Taylor, 2006; Miyazaki et al., 2006).

Lately, a number of reports on significantly increased storage stability of amorphous drugs in formulations with different silicates have been published. By grinding and quench-melting indomethacin with silica particles (Aerosil 200), Watanabe et al. (2001) showed that the storage stability of the formed amorphous dispersion was increased compared to the neat amorphous drug. It was found that only about 10% of the amorphous dispersion had

* Corresponding author at: Box 580, SE-751 23 Uppsala, Sweden.
Tel.: +46 018 471 4662; fax: +46 018 471 4377.
E-mail address: denny.mahlin@farmaci.uu.se (D. Mahlin).

0378-5173/$ – see front matter © 2011 Elsevier B.V. All rights reserved.
doi:10.1016/j.ijpharm.2011.02.031

been crystallizing after 60 days of storage, compared to 100% of the neat amorphous drug. Similar effects have later been observed when using 6 pharmaceutical silicates (Neusilin US2, Veegum-F, Florite-F, calcium silicate, kaolin, and Aerosil 200) (Bahl et al., 2008) and when spray-drying indomethacin with Aerosil 200 (Takeuchi et al., 2005). In these studies, the role of interactions between the amorphous component and the surface of the dispersed particles for stability was discussed. It seems like dispersed particles, which expose large enough surface area when dispersed in an amorphous phase, increase the physical stability by reducing molecular mobility by interaction with the surface (Watanabe et al., 2001). In polymer science the ability of filler particles to rigidify polymers has been known and studied (Wu, 1985; Fragiadakis et al., 2005; Crosby and Lee, 2007) and the existence of rigid amorphous phases in semi-crystalline low molecular weight compounds has been suggested (Craig et al., 2001). Kearns et al. (2008) have shown that when amorphous indomethacin and 1,3,5-(tris)-naphtylbenzene are formed on a solid substrate, a highly stable amorphous form of the compounds is obtained.

In a preliminary study we observed that glass particles in a size-range around 10 μm can increase the physical stability of amorphous sucrose when freeze-dried together. This was unexpected since it can be assumed that micro-sized filler particles do not expose a surface area large enough to have an impact on molecular mobility of the surrounding amorphous phase. However, it could not be excluded that the increased stability was imposed by other mechanisms such as crystallization inhibition of a dispersed phase (Molinuevo et al., 1998) and buffering effects of the included particles (Stubberud and Forbes, 1998).

The aim of this study was to find out if particles in the lower micro-range size can have an effect on physical stability of an amorphous disaccharide. For this we employed a freeze-dried model system based on commonly used excipients and a poorly soluble drug with various properties, e.g., crystallinity, hygroscopicity, hydrophobicity and surface area, as micro-sized filler particles and sucrose as the amorphous component. The idea was to evaluate the significance of the particle properties for the physical stability of freeze-dried particle/sucrose material. In the presentation of the studied system below, we use the terminology 'filler particles' for the added micro-sized filler particles and 'composites' for the produced freeze-dried materials.

2. Experimental

2.1. Materials

Sucrose (≥99.5% (GC), Sigma–Aldrich, St. Louis, MO, USA) was used to prepare 20% (w/w) solutions using de-ionized water as solvent. The pharmaceutical micro-sized filler particles, i.e., microcrystalline cellulose (Ph. Eur., MCC, Avicel®, FMC BioPolymer, Brussels, Belgium), starch from rice (Sigma–Aldrich, Belgium), talc (Ph. Eur., Apoteket Produktion & Laboratorier, Gothenburg, Sweden), calcium carbonate (Ph. Eur., $CaCO_3$, Apoteket Produktion & Laboratorier, Gothenburg, Sweden) and oxazepam (Wyeth, Münster, Germany), was used for preparing the composites.

2.2. Sample preparation

2.2.1. Fractionation and washing of filler particles

The excipient particles were classified using an Alpine 100-MZR laboratory air-classifier (Augsburg, Germany) using rotor speeds of 8000 and 12,500 rpm giving air-flow rates of 31–37 m^3/h. The collected fractions were washed twice by suspending them in filtrated (0.2 μm membrane filters, Millipore, Billerica, MA, USA) sucrose solution for 1 h in an ultrasonic bath, followed by centrifugation at 273 × *g* for 20 min and removing the supernatants. The centrifugations were done in an F0685 rotor in a Beckman Avanti 30 compact centrifuge (Palo Alto, CA, USA).

2.2.2. Suspension preparation

After washing, the filler particles were once again suspended in the sucrose solution in the same manner as when washing the filler particles. The suspensions were prepared to make the final dried product to consist of 40% (v/v) excipient particles, under the assumption that the powder density of amorphous sucrose was 1.5 g/ml (Elversson et al., 2007). The suspensions were freeze-dried.

To make sure that the stability of the amorphous phase was not affected by partially dissolved filler particles or impurities possibly released during the freezing process, sucrose solutions from which the particles had been removed prior to freeze-drying were prepared. A fraction of each suspension was freeze-thawed and centrifuged before the supernatants were freeze-dried.

2.2.3. Freeze-drying

Freeze-drying was performed in a pilot plant freeze-dryer (Lyostar II, FTS Kinetics, Stone Ridge, NY, USA). 7 ml vials (Pharma-Pack, Södertälje, Sweden) with a final fill volume of 1.0 ml were used. Freezing was performed by immersing the vials in ethanol mixed with dry ice for 2 min and putting them into the pre-cooled (−50 °C) freeze-dryer for 1 h. The pressure was then decreased to 5.3 Pa and shelf temperature increased to −20 °C at 5 °C/min, for primary drying for 1500 min. Secondary was performed by increasing the shelf temperature stepwise to −5, 0, 5, 10, 20 °C. Equilibration time at each step was 120 min and heating rate in between 5 °C/min. The program was then held at −4 °C and 13.3 Pa. Vials were sealed in the dryer under vacuum (13.3 Pa) and moved to −20 °C while waiting for the analyses. No visible structural collapse was detected in any of the vials and the dried material was of highly porous structure. Samples were prepared in triplicates.

2.3. Particle characterization

2.3.1. Permeametry

Blaine permeametry was used to determine the external surface area of the filler particles. It was calculated using a slip flow corrected Kozeny–Carman equation (Alderborn et al., 1985). Reported results are the mean of three separate experiments with three recordings of flow time for each experiment.

2.3.2. Gas adsorption

The specific surface area of the filler particles was measured using nitrogen gas adsorption (ASAP 2010, MicroMetrics, Londonderry, NH, USA) and calculated according to the BET equation (Brunauer et al., 1938). Reported results are the mean of two experiments.

2.3.3. Helium pycnometry

The apparent particle densities of the filler particles were determined with a helium pycnometer (AccuPyc 1330, MicroMetrics, Londonderry, NH, USA). Each sample was measured in three separate experiments with 10 cycles for each experiment.

2.3.4. Gravimetric vapour sorption

The moisture sorption as a function of relative humidity (RH) for the filler particles was recorded using a Symmetric Gravimetric Analyzer (SGA-100, VTI Corporation, Hialeth, FL, USA). Samples weighing 9–11 mg were analyzed with humidity varied between 10 and 80% RH at 25 °C in steps of 5% RH after drying the sample at 60 °C in dry gas until weight equilibrium. A weight change less than 0.02% (w/w) in 1 min was used as the equilibrium criteria.

2.3.5. Light microscopy

The filler particle size was estimated using an optical light microscope (Olympus BX51, Tokyo, Japan) equipped with a CCD camera (Olympus DP50, Tokyo, Japan). The filler particles were suspended in water to prevent agglomeration. Approximately 300 particles per filler particle type were measured on the length and the width using the Olympus DP-soft (Tokyo, Japan) software.

2.4. Solid state characterization

2.4.1. X-ray diffraction

Samples were analyzed using a Kratky camera (Hecus X-ray systems, Graz, Austria) for 7 h in a vacuum using Cu Ka-generated X-rays (of wavelength 1.542 Å) provided by an X-ray generator (Philips, PW1830/40, the Netherlands) operated at 50 kV and 40 mA. Diffracted X-ray was detected with a linear position-sensitive detector (MBraun, Garching, Germany) with a detector channel width of 0.0102° in a limited range of detection ($18.5° < 2\theta < 26.5°$). Every sample was analyzed once.

2.4.2. Differential scanning calorimetry

An SII DSC6200 (Seiko Instruments Inc., Chiba, Japan) was used for thermal analysis. The DSC was calibrated for heat flow and temperature using high purity indium. Nitrogen was used as purge gas at a constant flow rate of 80 ml/min. After drying at 50 °C for 10 min the samples weighing 1–6 mg were analyzed for crystallization temperature (T_{cr}) by heating at 5 °C/min from 0 °C to 220 °C. The samples were also analyzed for glass transition temperature (T_g) after drying at 80 °C for 5 min followed by a temperature scan at 40 °C/min from −40 °C to 150 °C. The measurements were done using standard aluminium pans (TA Instruments, New Castle, DE, USA) with pin-holed lids. All samples were analyzed in duplicates. The T_{cr} was taken to the onset temperature of the crystallization and the T_g was taken to the midpoint of the transition.

Layered samples of filler particles and pure freeze-dried sucrose were prepared by placing the filler particles (talc and oxazepam) in the bottom of the DSC standard aluminium pans with sucrose on top of the filler particles. Same proportions of the compounds were used as in the freeze-dried composites.

Humidified samples of the composites were analyzed in DSC at 5 °C/min from −20 °C to 220 °C after equilibration in 11% RH and 22% RH for 15–20 h at room temperature (22 °C). These samples were analyzed in the hermetic aluminium pans without pin-holes.

Due to poor baseline stability and relatively large change in heat capacity (ΔC_p) during crystallization, a standard linear background subtraction was not appropriate when analyzing the crystallization peak. Therefore, the baseline (*BL*) under the peak was described by the quasi-empirical equation

$$BL(T) = [a \cdot (T - b)^2 + c] + [\Delta C_p \cdot f_{cryst}(T)] \quad (1)$$

where the quadratic expression in the first square bracket could, by appropriate choice of the parameters *a*, *b* and *c* be fitted to the background, i.e., the calorimeter curve at temperatures below and above the peak. The expression in the second square bracket is the crystallization contribution to the baseline and assumed equal to the change in heat capacity (ΔC_p) times fraction crystallized ($f_{cryst}(T)$). $f_{cryst}(T)$ was determined by

$$f_{cryst}(T) = \frac{A_f(T)}{A_{peak}} \quad (2)$$

where $A_f(T)$ is the integral between the heat flow signal and the baseline (*BL*) from a temperature below the peak to the temperature *T*, and A_{peak} is the total integral (*T* is a temperature above the peak). Thus, one can see that there is a circular dependence between $f_{cryst}(T)$ and the baseline equation and the expression for

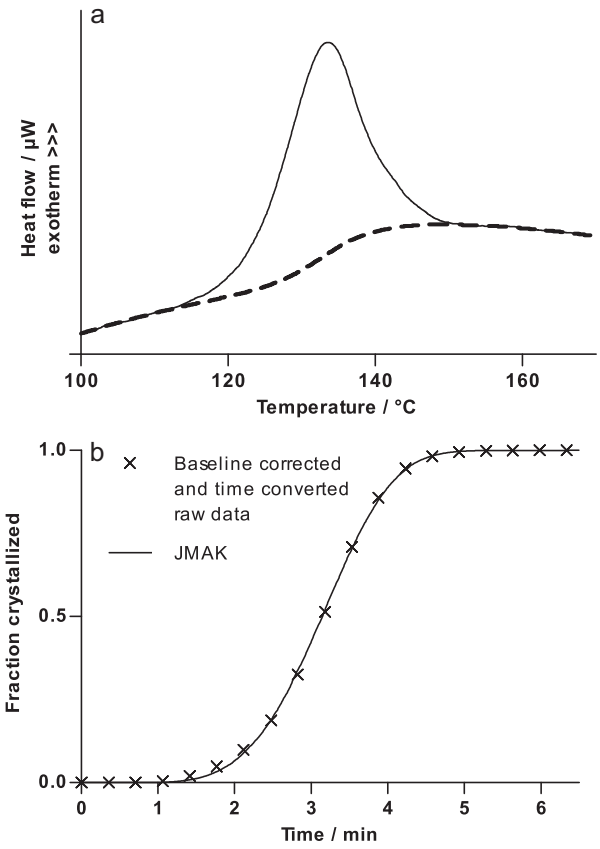

Fig. 1. (a) Crystallization peak from DSC experiment. Solid line is raw data and the dashed line indicates background calculated from Eq. (1). (b) The fraction crystallized $f_{cryst}(T)$ was determined from Eq. (2) and plotted as function of time and the JMAK equation (solid line) was fitted to the data points (crosses).

$f_{cryst}(T)$ is non-analytical. The baseline equation as well as $f_{cryst}(T)$ was, therefore, determined by an iterative process using Eqs. (1) and (2), ending when $f_{cryst}(T)$ became self-consistent. As start approximation the $f_{cryst}(T)$ was assumed to be zero at temperatures below the mid peak temperature and 1 above the mid peak temperature. The obtained baseline was subtracted from the raw data (Fig. 1a). The temperature was converted to time (t) by division by the heating rate and setting $t = 0$ at crystallization onset. Subsequently, f_{cryst} was plotted as a function of time and fitted to the Johnsson–Mehl–Avrami–Kolomogorov (JMAK) equation (Avrami, 1940):

$$f_{cryst}(t) = 1 - e^{-(kt)^m} \quad (3)$$

keeping the exponent *m* constant at 4, whereby the rate constant *k* was obtained (Fig. 1b).

2.4.3. Microcalorimetry

The moisture-induced isothermal (25 °C) crystallization of the samples at 33% RH and 43% RH was investigated using a microcalorimeter (2277 Thermal Activity Monitor, Thermometric AB, Järfälla, Sweden) according to method described in Sebhatu et al. (1994). About 15 mg sample was weighted into a 3 ml glass ampoule. A micro test tube containing a saturated salt solution was added to the vial which was sealed. The vial was lowered in the isothermal microcalorimeter and allowed to equilibrate for 30 min before thermal monitoring commenced. Monitoring was stopped once the thermal event had occurred and the baseline returned to zero. The samples were analyzed in duplicates.

A cubic background was fitted to the crystallization peak. The rate constant *k* was obtained by fitting the baseline subtracted data

(from Eq. (2)) to Eq. (3) keeping the exponent m constant at 4. The crystallization time (t_{cr}) was taken as the time where 50% of the crystallization peak area had evolved.

3. Results and discussion

3.1. Filler particle characteristics

The filler particles, four commercially available pharmaceutical excipients, and one poorly soluble drug, were selected to possess different properties expected to influence amorphous stability in different ways. To be able to produce the intended particle-sucrose composites, the particles needed to be dispersible but insoluble in water. Of the ones chosen (Table 1), starch and MCC are both hygroscopic and partially amorphous polymeric carbohydrates. Oxazepam is a crystalline hydrophobic drug. Talc and $CaCO_3$ are inorganic, crystalline particles. The filler particles were air classified to obtain powders with approximately similar size ranges. The results from the subsequent surface area characterization by Blaine permeametry and BET-surface gas adsorption are displayed in Table 1 where also the data from estimation of particle size by light microscopy can be found. Apparent from these results is the variation in particle size but within a relative narrow range with the median spanning from 1.3 to 4.7 μm.

3.2. Solid state structure of freeze-dried composites

After freeze-drying of the sucrose with and without the filler particles, all samples appeared to be porous white cakes without any visible signs of collapse. The X-ray spectra had diffuse background scattering with no or nearly indistinguishable diffraction peaks visible at diffraction angles typical for crystalline sucrose, thereby indicating that the sucrose of all samples was completely or nearly completely amorphous. The small traces of crystalline sucrose were found randomly among replicates of all the different samples with and without filler particles. To find out if the traces of sucrose crystallinity had an influence on the stability, an evaluation of correlations between stability and presence of crystalline traces was done. However, in no case could differences in stability be contributed to this parameter. Hence we conclude that the traces of crystallinity detected in some samples did not influence the results. As expected, when crystalline filler particles ($CaCO_3$, oxazepam and talc) were present in the samples they gave rise to diffraction peaks which overlapped the positions of the peaks obtained for the pure filler particles.

3.3. Heat-induced crystallization

All DSC thermograms obtained by heating at 5 °C/min had the same general pattern with thermal events ascribed as being a weak glass transition, crystallization, and melting (Fig. 2a). When measurements were made on filler particles alone, without the amorphous sugar present, no transitions could be detected below 200 °C. Hence, the detected transitions of the composites could be attributed to transitions of the amorphous sucrose.

The crystallization temperature (T_{cr}) of the freeze-dried mixtures were determined and used as an indicator of stability. All composites had significantly higher T_{cr} compared to sucrose alone (one-way ANOVA, Tukey *post hoc* test, $p < 0.05$, Fig. 3 and Table 2). The talc particles had the largest impact, raising the T_{cr} to 124 °C compared with 90 °C for sucrose alone.

Additional experiments were made to find out if the observed increase in T_{cr} was due to the filler particles affecting the heat conduction during the DSC measurement. A layer of filler particles was put in the bottom of a DSC pan and a layer of pure freeze-dried sucrose placed on top. In this manner each type of filler particle was layered with sucrose and run in the same way as the composite samples. The shape and T_{cr} of the layered samples did not differ from pure sucrose. These results lead us to conclude that the filler particles do not obstruct the heat flow and the detected raises in transition temperatures are not due to altered heat conduction of the samples.

Further, although the materials used as filler particles are insoluble in water, it could not be excluded that contaminants or fractions

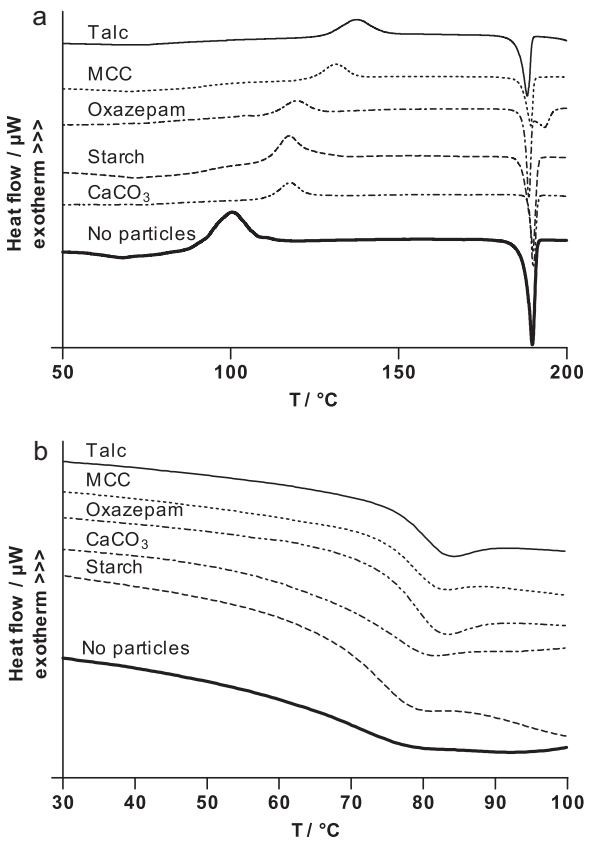

Fig. 2. (a) Typical DSC thermograms of the composites indicating exothermic crystallization peak and endothermic melting peak measured at 5 °C/min and (b) typical DSC thermograms indicating the endothermic shift being the glass transition of the composites measured at 40 °C/min.

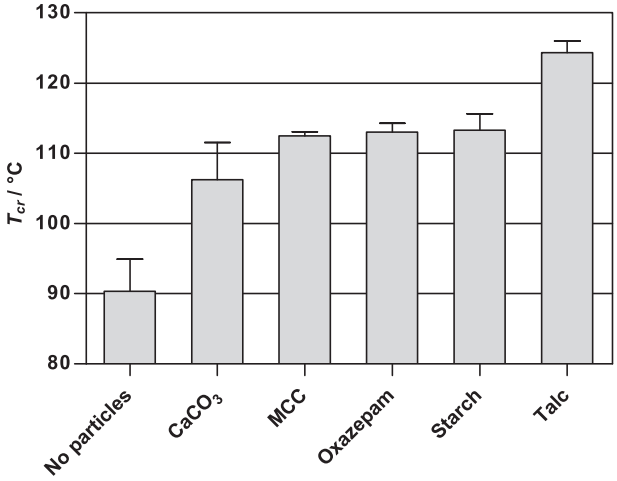

Fig. 3. Crystallization temperature (T_{cr}/°C) measured with DSC. All the composites have significantly higher T_{cr} compared to pure sucrose ($p < 0.05$, one-way ANOVA, Tukey *post hoc* test). Error bars indicate standard error of mean (SEM).

Table 1
Characteristics of the filler particles.

Filler particles	$CaCO_3$	MCC	Oxazepam	Starch	Talc
Surface area/(m^2/g)					
BET[a]	0.52	3.40	2.71	1.12	5.80
Blaine slip flow[b]	0.60 ± 0.01	2.4 ± 0.06	2.2 ± 0.4	1.5 ± 0.01	5.5 ± 0.06
Particle diameter/μm[c]	1.3 ± 1.3	3.2 ± 1.5	4.3 ± 1.5	4.7 ± 1.0	2.3 ± 1.4
Density/(kg/m^3)[b]	2.716 ± 0.002	1.585 ± 0.011	1.436 ± 0.004	1.529 ± 0.003	2.828 ± 0.007
Chemical formula	$CaCO_3$	$(C_6H_{10}O_5)_n$	$C_{15}H_{11}ClN_2O_2$	$(C_6H_{10}O_5)_n$	$Mg_3Si_4O_{10}(OH)_2$
Crystalline?	Yes	Semi	Yes	Semi	Yes
Hygroscopic?	No	Yes	No	Yes	No

[a] Values represent mean.
[b] Values represent mean ± SEM.
[c] Values represent median ± quartile deviation.

Table 2
Crystallization parameters measured with DSC at 5 °C/min (0% RH).

Filler particles	No particles	$CaCO_3$	MCC	Oxazepam	Starch	Talc
T_{cr}/°C	90.3 ± 4.6	106.3 ± 5.3*	112.5 ± 0.6*	113.0 ± 1.3*	113.3 ± 5.8*	124.3 ± 1.7*
k/min^{-1}	0.301 ± 0.026	0.290 ± 0.035	0.220 ± 0.018	0.323 ± 0.016	0.329 ± 0.021	0.231 ± 0.012

Values represent mean ± SEM.
* $p < 0.05$, one-way ANOVA, Tukey *post hoc* test.

of the filler particles were dissolved during preparation of feed dispersions for freeze-drying. If such components are incorporated into the amorphous phase it may have an effect on its T_g and T_{cr}. To assure that possible dissolved components were not the reason behind the increase in transition temperatures, new samples were prepared from freeze-thawed dispersions where the filler particles had been removed from the liquid before freeze-drying. These samples being free from filler particles but containing any possibly-dissolved components were analyzed by DSC in the same conditions as the samples with filler particles. All thermograms displayed similar T_{cr} as the samples without filler particles; no statistically significant differences in T_{cr} could be detected. These results imply that the significant difference in transition temperatures between sucrose with and without filler particles cannot be explained by contaminated samples or partially dissolved filler particles.

Table 2 shows the crystallization kinetic parameters determined from the fitting of the JMAK equation to the DSC crystallization data for the different composites. Although JMAK is derived for isothermal crystallizations, we applied it on the DSC-data to get an estimate of the rate constant, k, and thereby of the crystallization rate. The obtained k-values from crystallization of the composites were not significantly different from pure sucrose (One-way ANOVA, Tukey *post hoc* test, $p < 0.05$). This shows that the microparticles generally do not affect the crystallization process once started, even though increasing the temperature where crystallization is initiated.

3.4. Glass transition temperature

The step change in the DSC thermogram detected at approximately 60 °C was ascribed being the glass transition. However, the magnitude of this base line shift was very small. To enable proper detection, the T_g measurements of all samples were conducted at a heating rate of 40 °C/min, which increased the magnitude of the step change (Fig. 2b). As for the crystallization measurements, the samples were run in pin-holed pans dried at 80 °C before starting the T_g determination. This was done to ensure that the glass transition was not affected by humidity or thermal history, i.e., alterations in the amorphous state due to differences in the formation of the amorphous phase. The T_g of the amorphous sucrose (Fig. 4), was 67 °C for the pure sucrose but significantly higher for all composites (One-way ANOVA, Tukey *post hoc* test, $p < 0.05$). The increase was highest in the composite with talc (11 °C) and lowest with starch (3 °C).

3.5. Humidity-induced crystallization

Upon exposure to 43% RH in a microcalorimeter, the composites containing $CaCO_3$ or oxazepam displayed the same t_{cr} as pure freeze-dried sucrose. However, the composites containing starch, MCC or talc particles showed significantly prolonged t_{cr} (Fig. 5). Hence, in the case of humidity-induced crystallization, the ability of the different filler particles to stabilize seems dependent on particle type. Interestingly, talc, that does not absorb moisture, clearly prolongs humidity-induced crystallization as effectively as the hygroscopic filler particles MCC and starch. Accordingly, the ability of filler particles to stabilize does not fully correlate with hygroscopicity (Fig. 6). When t_{cr} was determined at a lower humidity, i.e., 33% RH, the samples containing $CaCO_3$ also had a significantly higher value compared with pure sucrose, but still, as in the case of 43% RH, oxazepam did not affect the amorphous stability (Fig. 7).

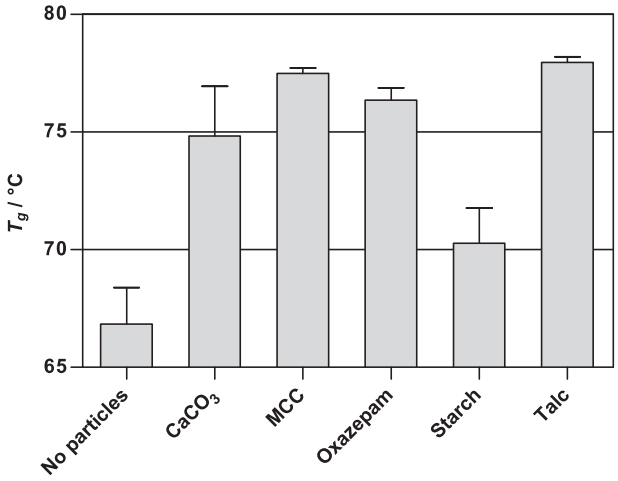

Fig. 4. Glass transition temperature (T_g/°C) measured with DSC. All the composites except the composite containing starch have significantly higher T_g compared to pure sucrose ($p < 0.05$, one-way ANOVA, Tukey *post hoc* test). Error bars indicate SEM.

Table 3
Crystallization parameters measured with MC at 43% RH.

Filler particles	No particles	$CaCO_3$	MCC	Oxazepam	Starch	Talc
t_{cr}/min	382.1 ± 6.353	379.6 ± 20.38	782.9 ± 58.19*	358.9 ± 18.91	637.2 ± 18.63*	780.6 ± 28.12*
k/(min^{-1} 10^{-3})	4.20 ± 0.18	6.25 ± 0.55*	1.99 ± 0.40*	5.83 ± 0.51	6.34 ± 0.42*	3.24 ± 0.53

Values represent mean ± SEM.
* $p < 0.05$, one-way ANOVA, Tukey *post hoc* test.

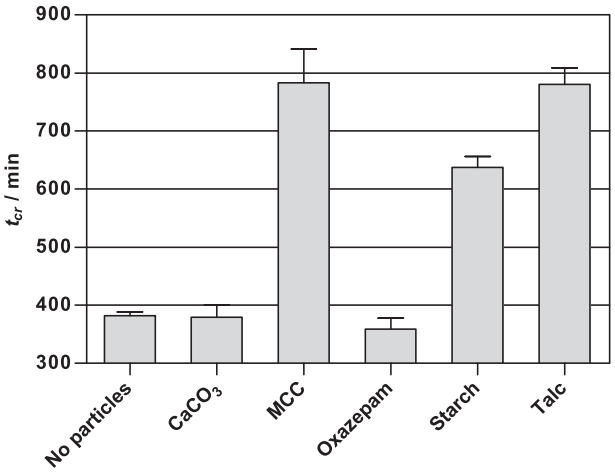

Fig. 5. Crystallization time (t_{cr}/min) measured with MC at 43% RH. The composites containing starch, MCC or talc have significantly higher t_{cr} compared to pure sucrose, while the composites containing $CaCO_3$ or oxazepam do not ($p < 0.05$, one-way ANOVA, Tukey *post hoc* test). Error bars indicate SEM.

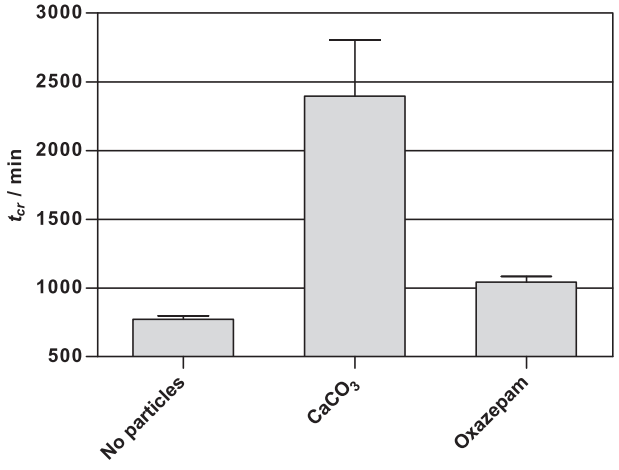

Fig. 7. Crystallization time (t_{cr}/min) measured with micro-calorimeter at 33% RH. The composite containing $CaCO_3$ has significantly higher t_{cr} compared to pure sucrose, while the composite containing oxazepam does not ($p < 0.05$, one-way ANOVA, Tukey *post hoc* test). Error bars indicate SEM.

Table 3 shows crystallization kinetics data determined from the fitting of the JMAK equation to the microcalorimeter crystallization data for the different composites. The composites containing $CaCO_3$ or starch have an increased crystallization rate, but the composite containing MCC has lowered crystallization rate. The composites containing oxazepam or talc were not significantly different from pure sucrose (one-way ANOVA, Tukey *post hoc* test, $p < 0.05$).

3.6. Crystallization temperature after equilibration with moisture

To further investigate how moisture affects stability in the freeze-dried composites, the samples containing $CaCO_3$, oxazepam and talc were equilibrated in 11% RH and 22% RH before hermetic sealing of the pans and analysis with DSC. As expected, the T_{cr} for pure sucrose was lowered after equilibration in moisture (Fig. 8).

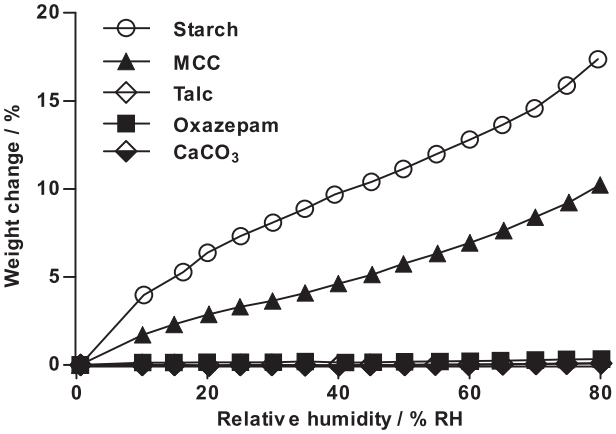

Fig. 6. Hygroscopicity of the filler particles measured using gravimetric vapour sorption. Starch and MCC are hygroscopic. Talc, oxazepam and $CaCO_3$ are not hygroscopic.

This was also the case for the examined composites. However, for the composites containing $CaCO_3$ or talc, the lowering in T_{cr} was less compared with pure sucrose. For the composite containing oxazepam, no difference in T_{cr} could be detected compared with pure sucrose, in other words the stabilizing effect of the particles was lost even at low levels of moisture in this composite.

The results from the humidity-induced crystallization suggest that there is a certain RH threshold for each filler particle type above which their stabilization effect is lost. Oxazepam can only inhibit crystallization in dry conditions as is evident from DSC measurements at dry conditions. Equilibration of the samples at a humidity as low as 11% make oxazepam loose its stabilizing ability, whereas

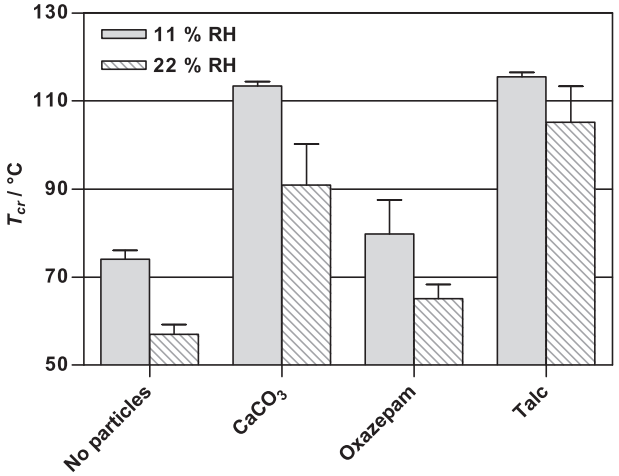

Fig. 8. Crystallization temperature (T_{cr}/°C) measured with DSC after equilibration in 11% RH and 22% RH for 15–20 h at room temperature. The composites containing $CaCO_3$ or talc have significantly higher T_{cr} compared to pure sucrose, while the composite containing oxazepam does not ($p < 0.05$, one-way ANOVA, Tukey *post hoc* test). Error bars indicate SEM.

$CaCO_3$ must be exposed to an RH of 43%. Talc, MCC, and starch delay crystallization at all humidity conditions examined in this study.

3.7. Discussion of possible stabilization mechanisms

The observation that incorporation of micro-sized filler particles into an amorphous disaccharide gives rise to increased physical stability has, to our knowledge, not been described previously. The mechanism behind the observed stabilizing effect from the filler particles is not apparent. The possibility that added particles in physical mixtures with amorphous lactose have the ability to buffer humidity during humidity exposure and subsequent crystallization has been discussed previously (Stubberud and Forbes, 1998). However, in our study the ability to stabilize against humidity-induced crystallization was independent of filler particle hygroscopicity. Also, the stabilization effect was significant for all particle types of filler particles at dry conditions in the DSC, where temperature is used as the stress factor to initiate crystallization. We therefore conclude that buffering of humidity or "internal desiccation" is not a major factor contributing to the increased stability of the composites.

It is worth noting that our original idea behind adding filler particles with various degrees of crystallinity was to evaluate if the presence of crystalline surfaces could alter the stability of the sucrose in terms of seeding of the amorphous phase. However, there were no indications that particles being partially amorphous (starch and MCC) influence the stability differently from the crystalline particles. Furthermore, it could be confirmed by X-ray that some of the samples contained traces of crystalline sucrose after freeze-drying and that these samples showed no difference in physical stability compared to those detected as fully amorphous. Hence, for the composite materials formed in this study where the volume fraction of incorporated particles is 40%, it seems like variations in heterogeneous nucleation is not something that can explain differences in crystallization kinetics.

When trying to understand the origin of the stabilization it has to be taken into consideration that addition of filler particles may impose alterations in the micro-structure of the amorphous phase. Although being highly porous on a micro-scale, freeze-dried amorphous disaccharides are forming an interconnected network throughout a sample (Liu, 2006). Incorporation of filler particles could potentially disperse the amorphous phase into isolated domains if the volume fraction of the particles is high enough. Furthermore, it is possible that a discontinuous micro-structure of this type can have an influence on the propagation of crystal growth. However, the results in our study do not support such a hypothesis since the rate of crystallization (k) seems fairly unaffected by the presence of micro-sized filler particles and an unaltered crystallization rate indicates that the crystallization propagation was unaffected. The only reduction in crystallization rate observed was for the composite with MCC at 43% RH. The reason for this observation is not obvious.

The possibility of a reduction in molecular mobility of the amorphous sucrose imposed by the micro-sized filler particles, in the same way as silica particles increase stability of amorphous indomethacin (Watanabe et al., 2001; Takeuchi et al., 2005; Bahl et al., 2008), cannot be excluded. The increase in T_g may be attributed to a decrease in the molecular mobility of the amorphous sucrose, attained by the presence of solid particles in the composites. The constant rate of crystallization for all composites at dry conditions, although occurring at different temperatures, is also supporting a reduced molecular mobility of the amorphous phase in the presence of micro-sized filler particles. This since, during heating in the DSC, the crystallization is observed at a temperature when the molecules have obtained high enough mobility for the transition to occur. Furthermore, it was also observed that the fillers with the larger surface area, i.e., talc, gave higher T_g and T_{cr}, and that $CaCO_3$, which has the smallest surface area, showed lowest increase in T_g and T_{cr}. This observation supports the view that the presence of solid particle surfaces affects the molecular mobility and, hence, the physical stability of the amorphous phase. It also implies that there are some interactions occurring between the sucrose and the solids surfaces, since otherwise the T_g of the amorphous phase would presumably be equal to the T_g of the pure amorphous sucrose. However, the difference in surface area is not large enough to fully confirm the validity of this hypothesis, as there were no strict correlations between surface area and stability. Hence, other factors, probably related to interactions between the surface and amorphous phase are also playing a role in these composites.

When the composites were exposed to humidity an interesting particle-specific phenomenon became apparent. The decline in ability to stabilize the amorphous phase for some materials at increasing RH indicates that the close contact, and interactions, between the amorphous phase and the particle surface is disrupted when water is absorbed into the system. The most humidity-sensitive filler particle was oxazepam, which makes sense since it is hydrophobic and was most difficult to disperse in water. A reasonable explanation for the loss in stabilization ability would hence be that when water is absorbed by the amorphous sucrose and becomes hydrated, it subsequently decreases its interaction with the hydrophobic surfaces of oxazepam. The stabilization ability is thereby lost.

It is somewhat unexpected that particles on the size-scale used in this study would provide surface area to enable a rigidification of the amorphous phase as nano-sized filler particles do. However, the data generated in this study suggest that this is the case also for filler particles in sizes below 10 μm.

4. Conclusion

Incorporation of micro-sized filler particles into freeze-dried amorphous sucrose evidently increased the physical stability of the amorphous phase. The stabilization was apparent from a delay in heat and moisture-induced crystallization. The increased stability could neither be attributed to moisture buffering effects nor possible alterations of the micro-structure of the amorphous phase. Since the stabilization was accompanied by an increase in T_g, the most likely explanation for the increased physical stability was a reduced molecular mobility of the amorphous phase, which would explain the decreased tendency for crystallization. Probably this rigidification of the amorphous phase is mediated by interactions between the amorphous sucrose and the filler particle surface. Moreover, this interaction, and hence stabilization effect, was impaired by sorption of water into the amorphous composites.

To our knowledge this work is the first example showing that micro-sized filler particles of various commonly used excipients can give amorphous materials higher physical stability. Particle-induced stabilization of amorphous materials has important implications, since many amorphous formulations often consist of several components and contain interfaces between micro-domains. In future work it is of interest to further study the enhanced physical stability of amorphous materials with filler particles by taking a deeper look at the surface interactions, the role of water, and to explore the applicability to various amorphous components and filler particles.

Acknowledgments

We wish to thank AstraZeneca for financial support (Young Researcher Grant, 2007). Johan Gråsjö, Department of Pharmacy,

Uppsala University, is gratefully acknowledged for development of DSC baseline correction method. We would also like to thank Sebastian Håkansson and Åsa Schoug, Department of Microbiology, Swedish University of Agricultural Sciences, for providing the freeze-dryer and for valuable discussions.

Appendix A. Supplementary data

Supplementary data associated with this article can be found, in the online version, at doi:10.1016/j.ijpharm.2011.02.031.

References

Alderborn, G., Duberg, M., Nyström, C., 1985. Studies on direct compression of tablets X. Measurement of tablet surface-area by permeametry. Powder Technol. 41, 49–56.
Avrami, M., 1940. Kinetics of phase change II. Transformation-time relations for random distribution of nuclei. J. Chem. Phys. 8, 212–224.
Bahl, D., Hudak, J., Bogner, R.H., 2008. Comparison of the ability of various pharmaceutical silicates to amorphize and enhance dissolution of indomethacin upon co-grinding. Pharm. Dev. Technol. 13, 255–269.
Berggren, J., Alderborn, G., 2003. Effect of polymer content and molecular weight on the morphology and heat- and moisture-induced transformations of spray-dried composite particles of amorphous lactose and poly(vinylpyrrolidone). Pharm. Res. 20, 1039–1046.
Bhugra, C., Pikal, M.J., 2008. Role of thermodynamic, molecular, and kinetic factors in crystallization from the amorphous state. J. Pharm. Sci. 97, 1329–1349.
Bhugra, C., Shmeis, R., Krill, S.L., Pikal, M.J., 2008. Prediction of onset of crystallization from experimental relaxation times II. Comparison between predicted and experimental onset times. J. Pharm. Sci. 97, 455–472.
Brunauer, S., Emmett, P.H., Teller, E., 1938. Adsorption of gases in multimolecular layers. J. Am. Chem. Soc. 60, 309–319.
Chatterjee, K., Shalaev, E.Y., Suryanarayanan, R., 2005. Raffinose crystallization during freeze-drying and its impact on recovery of protein activity. Pharm. Res. 22, 303–309.
Craig, D.Q.M., Kett, V.L., Murphy, J.R., Price, D.M., 2001. The measurement of small quantities of amorphous material—should we be considering the rigid amorphous fraction? Pharm. Res. 18, 1081–1082.
Crosby, A.J., Lee, J.Y., 2007. Polymer nanocomposites: the "nano" effect on mechanical properties. Polym. Rev. 47, 217–229.
Elversson, J., Andersson, K., Millqvist-Fureby, A., 2007. An atomic force microscopy approach for assessment of particle density applied to single spray-dried carbohydrate particles. J. Pharm. Sci. 96, 905–912.
Fragiadakis, D., Pissis, P., Bokobza, L., 2005. Glass transition and molecular dynamics in poly (dimethylsiloxane)/silica nanocomposites. Polymer 46, 6001–6008.
Graeser, K.A., Patterson, J.E., Rades, T., 2008. Physical stability of amorphous drugs: evaluation of thermodynamic and kinetic parameters. J. Pharm. Pharmacol. 60, 116.
Hancock, B.C., Parks, M., 2000. What is the true solubility advantage for amorphous pharmaceuticals? Pharm. Res. 17, 397–404.
Hancock, B.C., Shamblin, S.L., Zografi, G., 1995. Molecular mobility of amorphous pharmaceutical solids below their glass-transition temperatures. Pharm. Res. 12, 799–806.
Izutsu, K., Kojima, S., 2002. Excipient crystallinity and its protein-structure-stabilizing effect during freeze-drying. J. Pharm. Pharmacol. 54, 1033–1039.
Kearns, K.L., Swallen, S.F., Ediger, M.D., Wu, T., Sun, Y., Yu, L., 2008. Hiking down the energy landscape: progress toward the Kauzmann temperature via vapor deposition. J. Phys. Chem. B 112, 4934–4942.
Konno, H., Taylor, S.L., 2006. Influence of different polymers on the crystallization tendency of molecularly dispersed amorphous felodipine. J. Pharm. Sci. 95, 2692–2705.
Lin, Y., Cogdill, R.P., Wildfong, P.L.D., 2009. Informatic calibration of a materials properties database for predictive assessment of mechanically activated disordering potential for small molecule organic solids. J. Pharm. Sci 98, 2696–2708.
Lindfors, L., Forssen, S., Skantze, P., Skantze, U., Zackrisson, A., Olsson, U., 2006. Amorphous drug nanosuspensions 2. Experimental determination of bulk monomer concentrations. Langmuir 22, 911–916.
Liu, J., 2006. Physical characterization of pharmaceutical formulations in frozen and freeze-dried solid states: techniques and applications in freeze-drying development. Pharm. Dev. Technol. 11, 3–28.
Mahlin, D., Berggren, J., Gelius, U., Engström, S., Alderborn, G., 2006. The influence of PVP incorporation on moisture-induced surface crystallization of amorphous spray-dried lactose particles. Int. J. Pharm. 321, 78–85.
Miyazaki, T., Yoshioka, S., Aso, Y., 2006. Physical stability of amorphous acetanilide derivatives improved by polymer excipients. Chem. Pharm. Bull. 54, 1207–1210.
Molinuevo, C.H., Mendez, G.A., Müller, A.J., 1998. Nucleation and crystallization of PET droplets dispersed in an amorphous PC matrix. J. Appl. Polym. Sci. 70, 1725–1735.
Murdande, S.B., Pikal, M.J., Shanker, R.M., Bogner, R.H., 2010. Solubility advantage of amorphous pharmaceuticals I. A thermodynamic analysis. J. Pharm. Sci. 99, 1254–1264.
Okumura, T., Ishida, M., Takayama, K., Otsuka, M., 2006. Polymorphic transformation of indomethacin under high pressures. J. Pharm. Sci. 95, 689–700.
Pehkonen, K.S., Roos, Y.H., Miao, S., Ross, R.P., Stanton, C., 2008. State transitions and physicochemical aspects of cryoprotection and stabilization in freeze-drying of *Lactobacillus rhamnosus* GG (LGG). J. Appl. Microbiol. 104, 1732–1743.
Planinsek, O., Zadnik, J., Kunaver, M., Srcic, S., Godec, A., 2010. Structural evolution of indomethacin particles upon milling: time-resolved quantification and localization of disordered structure studied by IGC and DSC. J. Pharm. Sci. 99, 1968–1981.
Roberts, C.J., Debenedetti, P.G., 2002. Engineering pharmaceutical stability with amorphous solids. AIChE J. 48, 1140–1144.
Rumondor, A.C.F., Stanford, L.A., Taylor, L.S., 2009. Effects of polymer type and storage relative humidity on the kinetics of felodipine crystallization from amorphous solid dispersions. Pharm. Res. 26, 2599–2606.
Schoug, Å., Mahlin, D., Jonson, M., Håkansson, S., 2009. Differential effects of polymers PVP90 and Ficoll400 on storage stability and viability of *Lactobacillus coryniformis* Si3 freeze-dried in sucrose. J. Appl. Microbiol. 99, 2032–2048.
Sebhatu, T., Alderborn, G., 1999. Relationships between the effective interparticulate contact area and the tensile strength of tablets of amorphous and crystalline lactose of varying particle size. Eur. J. Pharm. Sci. 8, 235–242.
Sebhatu, T., Angberg, M., Ahlneck, C., 1994. Assessment of the degree of disorder in crystalline solids by isothermal microcalorimetry. Int. J. Pharm. 104, 135–144.
Shamblin, S.L., Huang, E.Y., Zografi, G., 1996. The effects of co-lyophilized polymeric additives on the glass transition temperature and crystallization of amorphous sucrose. J. Therm. Anal. 47, 1567–1579.
Stubberud, L., Forbes, R.T., 1998. The use of gravimetry for the study of the effect of additives on the moisture-induced recrystallisation of amorphous lactose. Int. J. Pharm. 163, 145–156.
Takeuchi, H., Nagira, S., Yamamoto, H., Kawashima, Y., 2005. Solid dispersion particles of amorphous indomethacin with fine porous silica particles by using spray-drying method. Int. J. Pharm. 293, 155–164.
Vromans, H., Bolhuis, G.K., Lerk, C.F., Vandebiggelaar, H., Bosch, H., 1987. Studies on tableting properties of lactose VII. The effect of variations in primary particle-size and percentage of amorphous lactose in spray-dried lactose products. Int. J. Pharm. 35, 29–37.
Watanabe, T., Wakiyama, N., Usui, F., Ikeda, M., Isobe, T., Senna, M., 2001. Stability of amorphous indomethacin compounded with silica. Int. J. Pharm. 226, 81–91.
Willart, J.F., Descamps, M., 2008. Solid state amorphization of pharmaceuticals. Mol. Pharm. 5, 905–920.
Wu, S., 1985. Phase structure and adhesion in polymer blends: a criterion for rubber toughening. Polymer 26, 1855–1863.
Ziffels, S., Steckel, H., 2010. Influence of amorphous content on compaction behaviour of anhydrous [alpha]-lactose. Int. J. Pharm. 387, 71–78.